J Solid State Electrochem (2011) 15:861–876
DOI 10.1007/s10008-010-1289-0

REVIEW

The isotope exchange depth profiling (IEDP) technique using SIMS and LEIS

John A. Kilner · Stephen J. Skinner · Hidde H. Brongersma

Received: 22 December 2010 / Accepted: 29 December 2010 / Published online: 5 February 2011
© Springer-Verlag 2011

Abstract The determination of the mass transport kinetics of oxide materials for use in electrochemical systems such as fuel cells, sensors and oxygen separators is a significant challenge. Several techniques have been proposed to derive these data experimentally with only the oxygen isotope exchange depth profile technique coupled with secondary ion mass spectrometry (SIMS) providing a direct measure of these kinetic parameters. Whilst this allows kinetic information to be obtained, there is a lack of knowledge of the surface chemistry of these complex processes. The advent of low-energy ion scattering (LEIS) now offers the opportunity of correlating exchange kinetics with chemical processes at materials atomic surfaces, giving unprecedented levels of information on electrochemical systems with isotopic discrimination. Here, the challenges of these techniques, including sample preparation, are discussed and the advantages of the combined approach of SIMS and LEIS illustrated with reference to key literature data.

Keywords SIMS · LEIS · Isotopic exchange · Electrochemical devices · SOFCs

J. A. Kilner · S. J. Skinner (✉) · H. H. Brongersma
Department of Materials, Imperial College,
London, UK
e-mail: s.skinner@imperial.ac.uk

H. H. Brongersma
Eindhoven University of Technology,
Eindhoven, the Netherlands

H. H. Brongersma
ION-TOF GmbH,
Heisenbergstrasse 15,
48149, Munster, Germany

Introduction

There is currently much interest in the study of ceramic oxide materials for applications in high-temperature electrochemical devices for clean energy technologies. Examples of these applications include solid oxide fuel cells (SOFCs) for electrical power generation, oxygen separation membranes for oxyfiring hydrocarbons, as part of a carbon capture and storage system, and solid oxide electrolysers for the production of hydrogen. Of major importance to all these applications is the study of the transport of oxygen in the active ceramic components, covering oxygen transport within the bulk of the materials, along and across grain boundaries or heterointerfaces, and across the gas–solid interface, i.e. the surface. There are a variety of methods that can be used to obtain this kinetic information however they all have their particular strengths and weaknesses. The method that has the simplest methodology (conceptually) but is perhaps the most difficult to execute is the so-called isotope exchange depth profiling (IEDP) method which yields oxygen tracer diffusion coefficients (D_T) and surface exchange coefficients (k) for oxide samples in single crystal, ceramic or thin film format. In the following sections, the IEDP technique will be described with the use of secondary ion mass spectrometry (SIMS) as the depth profiling technique. To illustrate the technique examples are taken from materials for applications in SOFCs and an extension of the technique will be discussed, involving the use of low-energy ion scattering (LEIS) to reveal detailed surface information about exchanged samples.

Methodology

The measurement of kinetic data, such as the diffusion coefficient, for solid-state materials is often carried out by

the use of tracer atoms. For many elements, this has involved the use of long lived radioactive isotopic tracers. A sample is prepared and the tracer is introduced by an appropriate method, this is then followed by an anneal under controlled conditions. The measurement of the resulting diffusion profile within the solid can take place by a number of methods; the most usual technique is by sectioning the sample and then measuring the activity of the slice. This procedure is very difficult to perform for oxygen because oxygen has only short-lived radioisotopes and so an alternative has to be used. Fortunately natural oxygen is composed of three stable isotopes, a majority isotope, oxygen 16 (99.76% natural abundance) with two minority isotopes oxygen 18 (0.20%) and oxygen 17 (0.04%). Oxygen 18 is most often used as a stable tracer for isotopic exchange experiments with oxide samples as it is readily available in highly enriched form. The IEDP technique consists of annealing an appropriate single crystal or ceramic sample in an ^{18}O enriched atmosphere for an appropriate time and then determining the depth profile by either direct depth profiling or by using a line scanning technique. Some precautions must be taken to ensure that the sample is of appropriate quality and these are mentioned below in "Preparation of samples for SIMS oxygen tracer diffusion analysis."

The samples for an exchange and diffusion experiment must be of sufficient size such that the diffusion fronts from all the surfaces of the sample do not meet in the centre. In this case a simpler form of the solution to the diffusion equation can be used corresponding to diffusion in a semi-infinite medium. The solution to the diffusion equation describing the isotopic fraction of oxygen 18 as a function of depth can be written in a form appropriate to the IEDP method in the following way.

$$C'(x,t) = \frac{C(x,t) - C_{bg}}{C_g - C_{bg}} = \mathrm{erfc}\left[\frac{x}{2\sqrt{Dt}}\right] - \left[\exp\left(\frac{kx}{D} + \frac{k^2 t}{D}\right) \times erfc\left(\frac{x}{2\sqrt{Dt}} + k\sqrt{\frac{t}{D}}\right)\right] \quad (1)$$

where $C(x, t)$ is the ratio of intensity of ^{18}O signal measured by SIMS to the total intensity of (^{18}O+^{16}O) in the material as measured by SIMS, x is the distance from the surface of the pellet and t is the time of the isotope exchange, C_{bg} is the natural isotopic background of ^{18}O (=0.002), C_g is the isotope fraction of ^{18}O in the gas during the ^{18}O exchange, D is the bulk oxygen tracer diffusion coefficient and k is the tracer surface exchange coefficient.

In order to obtain the kinetic parameters D and k, experimental profiles are fitted to Eq. 1 using a non-linear least squares method. A particularly fine example of the quality of data that can be obtained is shown in Fig. 1 for a ceramic sample of the mixed conductor $La_{0.6}Sr_{0.4}Co_{0.2}Fe_{0.8}O_{3-\delta}$, annealed in an enriched oxygen atmosphere at 854 °C.

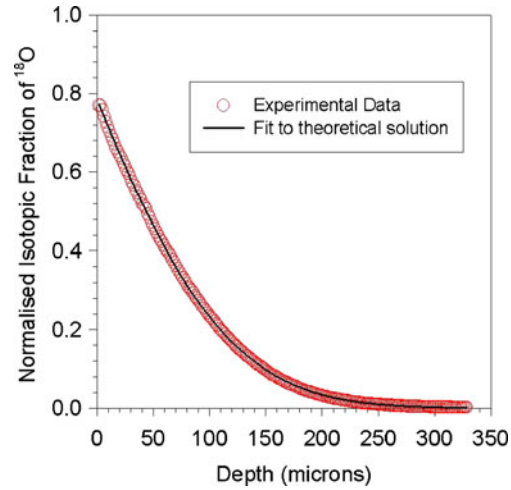

Fig. 1 ^{18}O diffusion profile of $La_{0.6}Sr_{0.4}Co_{0.2}Fe_{0.8}O_{3-d}$. The sample was annealed at 854 °C for 754 s at a pO_2 of 1,000 mbar. $D^*=7.4\times10^{-8}$ cm^2/s, $k=2.4\times10^{-5}$ cm/s

Equation 1 can be rewritten in terms of two dimensionless parameters x' and h' that are defined below;

$$x' = \frac{x}{2\sqrt{Dt}}, \text{ and } h' = \frac{k}{D}\sqrt{Dt} \quad (2)$$

$$C'(x,\ t) = \mathrm{erfc}(x') - \left\{\exp\left(2x'h' + h'^2\right)\mathrm{erfc}(x' + h')\right\} \quad (3)$$

This equation defines a family of normalised penetration profiles that can be viewed in three dimensions as the surface shown in Fig. 2. An interesting part of this curve is the plane defined by $x = 0$, i.e. at the surface of the sample. In this case, Eq. 3 reduces to

$$C'(0,\ t) = 1 - \exp\left(h'^2\right)\mathrm{erfc}(h') \quad (4)$$

This shows how the normalised surface isotopic fraction grows as a function of the anneal time for a fixed temperature (i.e. D and k). This expression can also be used to check the validity of the solutions obtained by the fitting described above by plotting the surface isotopic fraction versus the values of h' obtained from a number of anneal experiments. Figure 3 shows an example of data from a number of anneals of $La_{0.6}Sr_{0.4}CoO_{3-\delta}$ where normalised surface concentration is plotted against h' [1].

Preparation of samples for SIMS oxygen tracer diffusion analysis

Sample preparation for oxygen diffusion analysis by SIMS is a critical step to ensure that accurate data are obtained, within the boundaries of the errors of the technique as

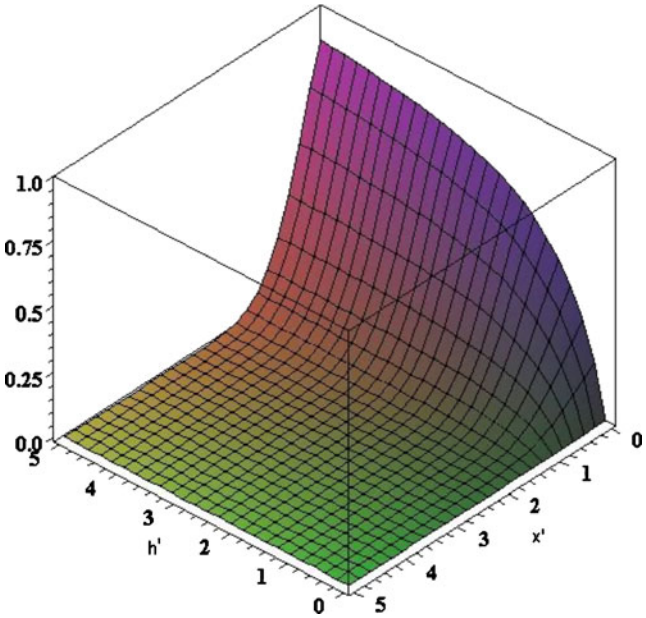

Fig. 2 The Normalised isotopic concentration as a function of the dimensionless variables h' and x'

discussed later. One of the key criteria in performing an ^{18}O exchange analysis is to ensure that the samples are sufficiently dense to ensure that only closed porosity is present. This is key, as it is essential that after an exchange the depth of the diffusion profile can be accurately determined. If there is any open porosity giving a pathway for oxygen penetration from an alternative direction then an artificial elevated isotopic concentration will result. Oxygen diffusion profiles can be successfully obtained from a variety of sample types, but most commonly polycrystalline samples are used. Successful examples of oxygen diffusion analysis have been reported for single crystals [2–5], thin films [6] and heterostructured layers [7, 8]. Indeed, use of alternative

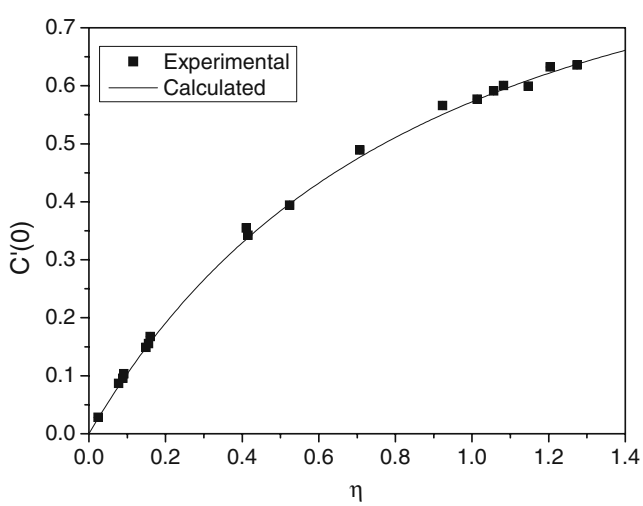

Fig. 3 Calculated and experimentally observed ^{18}O surface fraction as a function of h'. From reference [1] where $\eta \equiv h'$

geometries such as single crystals can facilitate the extraction of anisotropic diffusion properties in materials.

To prepare polycrystalline samples for exchange and diffusion analysis, it is essential that the starting material is a finely divided powder that has a high degree of sinterability. This ensures that on suitable sintering an overall density of greater that 95% of the theoretical density of the material will be achieved. As well as high sinterability it is likely that the material will require uniaxial and/or isostatic pressing to aid the sintering process. Of course sample size is also an important parameter and is influenced by the likely diffusion length of the tracer used (sample thickness) and the dimension of the sample holders for the instrument used for the analysis. Polycrystalline samples used are typically discs of 10–13 mm diameter with a thickness of 1–2 mm although, as will be discussed, alternative geometries are possible. Having selected an appropriately sized sample for the isotopic exchange there are a number of other criteria that have to be satisfied for a successful SIMS analysis. A full discussion of the details of choosing the appropriate boundary conditions for the exchange experiment is given by De Souza and Chater [9] and of the complexities of extraction of kinetic parameters by De Souza and Martin [10]. As described elsewhere the conditions used in the isotopic exchange experiment are critical, and it is essential that a long equilibration anneal is performed in a pure (99.999%) $^{16}O_2$ environment prior to the isotopic exchange anneal. Furthermore, the sample has to be rapidly heated and subsequently quenched to ensure that the diffusion profile is that of the tracer at the temperature of interest. If this step is not correctly performed, it is likely that artefacts will appear in the diffusion profile that could lead to misinterpretation of diffusion phenomena, such as grain boundary tailing.

Nernst equation: calculated diffusion coefficient, conductivity

Before an exchange anneal can be carried out the approximate depth of the penetration profile should be calculated. This is essential to ensure that the obtained diffusion profile is clearly within either the depth profile (<10 μm) or line scan (>50 μm) regime. Diffusion profiles lying between these regimes cannot be reliably analysed. A good approximation, particularly in pure oxide ion conductors, can be obtained from the Nernst equation, relating the measured conductivity to the diffusion coefficient.

$$D = \frac{kT\sigma}{Nq^2} \tag{5}$$

where D=tracer diffusion coefficient, k=Boltzmann constant, T=temperature, σ=conductivity, q=charge and N= number of anions/unit volume.

To achieve a reliable depth profile, it is essential that the surface is well defined and hence after sintering further sample preparation is required. Fully dense polycrystalline materials have to be polished to a mirror finish. Normally, this sample preparation is achieved using a combination of SiC grinding media followed by successively finer grades of diamond suspension usually to a 0.25 μm finish. This gives a relatively low surface roughness. Of course polishing with SiC and diamond media, and the associated sample mounting introduces potential contamination. Careful cleaning and sample handling is therefore required. Commonly contaminants such as Na, K, F and Cl amongst others are observed when careful sample handling has been neglected. One further note on sample quality, for samples with a low value of the bulk or lattice diffusion coefficient, care must be taken to remove the effects of surface damage introduced during any polishing steps.

Furthermore, difficulties with sample preparation are introduced when considering the nature of the sample to be analysed. As discussed earlier, there are two kinetic parameters that can be extracted from an isotopic exchange and SIMS analysis—tracer diffusion and surface exchange coefficients. The surface exchange process in oxides is normally an oxygen reduction and incorporation reaction, Eq. 6, which is frequently a rate limiting step.

$$O_{2(g)} + 2\,e \;\rightarrow\; O^{2-} \tag{6}$$

In electrical insulators, such as SOFC electrolytes, this process is negligible in a dry oxygen atmosphere. It is therefore necessary to introduce the tracer in an alternative way: either through the use of labelled H_2O or through coating the sample surface with an oxygen reduction catalyst such as Ag or Pt. Of course introducing a surface layer presents a number of challenges, not least of which is that the measured surface exchange coefficient is no longer that of the sample. Using labelled water overcomes this issue but may introduce protonic species to the sample. With mixed conductors this is typically not a problem as the surfaces are frequently active towards surface reduction and exchange. These issues will be reflected in the type of diffusion profile obtained.

Once a sample has been isotopically exchanged there are two potential methods for the subsequent SIMS analysis: depth profiling and line scanning. Each of these techniques has advantages and are typically used in cases with very different diffusion kinetics and will be discussed in turn.

Depth profile analysis of oxygen diffusion profiles

Depth profile analysis is perhaps the simplest and most common method of determining oxygen diffusion profiles in ceramic samples. In this mode the exchanged sample is loaded into the SIMS analysis chamber on a sample holder alongside a sample of the same nominal composition but unexchanged. The purpose of loading these two samples simultaneously is so that the background concentration of the isotope can be accurately determined. The depth profile analysis consists of sputtering an area of the sample using a raster scan. In this type of analysis the area to be sputtered, the gun to be used and the species to be analysed are carefully determined. These parameters are also instrument specific and vary depending on the instrument used. For instance when using a quadrupole system only certain selected species will be analysed, whereas with a time-of-flight (ToF) system all mass species are automatically collected and individual species subsequently analysed using appropriate software.

One of the main limitations of the depth profile technique is in the depth of crater that can be successfully sputtered in a reasonable timescale. Typically, a crater depth of 1–2 μm can be readily sputtered in a matter of a few hours and this is acceptable for materials that have slow diffusion kinetics. The crater depth can easily be tuned through careful selection of the exchange anneal time and temperature, but for many materials, irrespective of this, a much longer diffusion profile is obtained. Frequently, this can be in excess of 100 μm, and in this case the depth profiling technique is inappropriate and should not be used. For these longer profiles a line scan technique should be considered, as discussed in "Line scan analysis of oxygen diffusion."

Typical diffusion profiles obtained by depth profiling from the $(La,Sr)MnO_3$ family of materials are shown in Fig. 4. Each of the datasets was recorded at different temperatures and hence the penetration depths displayed on the *x*-axis vary slightly. Note that the maximum of the *x*-axis is 2.0 μm, well within the range required for a depth profile measurement. It is also of interest to note that the isotopic concentration (*y*-axis) is not fixed at a constant value, and in this case is actually rather high at between ~75–100%. It is also clear from these data that the fit of the Crank solution to Fick's law to the experimental data is not ideal, and highlights one of the features of these measurements—the influence of grain boundaries.

Whilst obtaining depth profiles from bulk polycrystalline samples is of considerable value for the analysis of both oxygen diffusion and surface exchange characteristics of isotropic electrochemical materials, there are an increasing number of anisotropic materials with differential diffusion coefficients, often by several orders of magnitude, determined by the sample crystallography. Efforts have therefore been made to analyse these anistropic systems through the use of both single crystal samples and thin film materials. Single crystals are frequently difficult to obtain, and hence

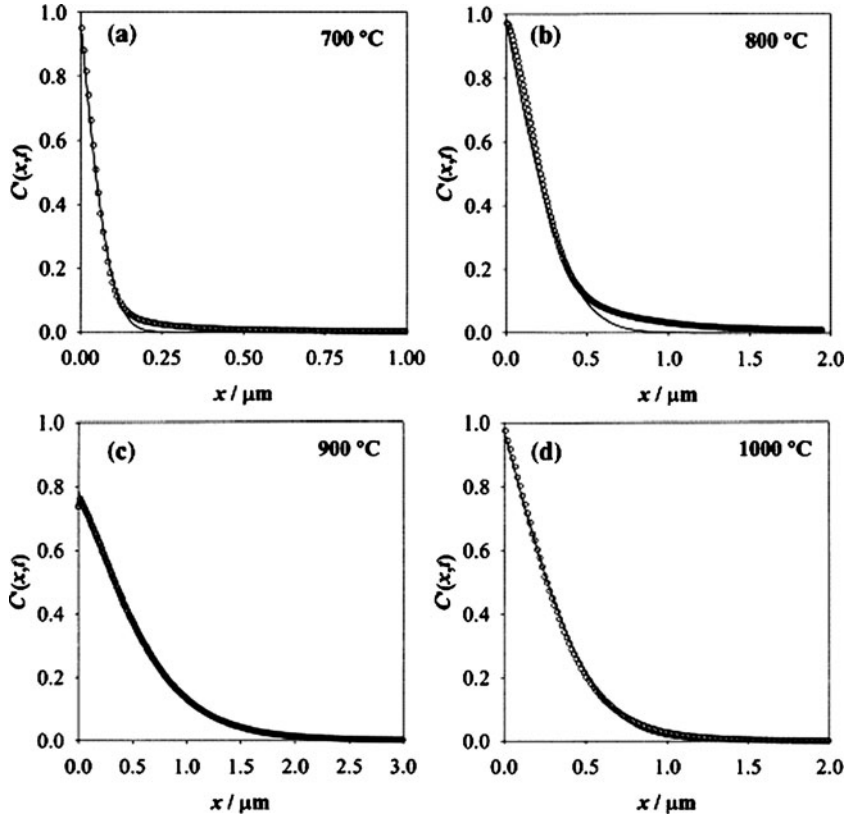

Fig. 4 Example ^{18}O depth profiles obtained from the mixed conducting oxide $La_{1-x}Sr_xMnO_{3\pm d}$ over the temperature range 700–1,000 °C. From De Souza et al. [65]

the application of thin film deposition techniques such as pulsed laser deposition and molecular organic chemical vapour deposition has led to advances in the determination of oxygen transport kinetics from these challenging materials. Burriel et al. [6] have pioneered a technique to extract both *a*–*b* plane and *c*-axis diffusion and exchange data from 400 nm thin films using a gold cap and combination of both depth profile and line scan approaches, as highlighted in Fig. 5. Here, the combination of short diffusion anneals and low temperatures enabled access to these parameters.

Line scan analysis of oxygen diffusion

In the case where a depth profile is not appropriate because of the diffusion length achieved a different mode of operation is used. In this mode, the sample is sectioned post-exchange, as detailed in Fig. 6. The cross sections are then also polished and cleaned as they would be for a depth profile. It is also critical that these sections are mounted together to ensure that the surface is clearly defined, as illustrated. Whilst the line scan technique is useful for fast ion conductors there are also some limitations. These are primarily related to the instrument specification as the quality of the data obtained depends to a large extent on the spot size of the beam being used. Typically, this is of the order of a few microns, and hence can introduce a significant uncertainty in the surface concentration of the isotopic species. This also gives a practical limitation for the minimum length of line scan that can be achieved. It is accepted that anything below ~50 µm will not produce reliable data. Typically, the line scan technique is required for those mixed conductors with fast surface exchange kinetics and oxygen diffusion, leading, in many cases to diffusion profiles of up to 7–800 µm.

A typical example of a line scan obtained from a 9.5% yttria stabilised zirconia (YSZ) single crystal is shown in Fig. 7, and it is immediately apparent through comparison with Fig. 4 that the penetration depth is significantly greater corresponding to the greater diffusion coefficient. With these two modes of analysis, it is clear that there are limitations with each, and hence the experiment requires careful consideration. Depth profiles are typically limited to relatively shallow crater depths of $\lesssim$10 µm, which is a practical limit considering the sputter time and the crater roughness resulting from the increased depth. With the line scan technique, the limit is that of the beam size, which produces a lower limit below which reliable data cannot be obtained. Typically, this is of the order of several microns giving a useful lower guide of ~50 µm with older generation instruments. More recently, the advent of nano-SIMS [11, 12] has meant that data can be obtained from individual grains by the depth profile technique with

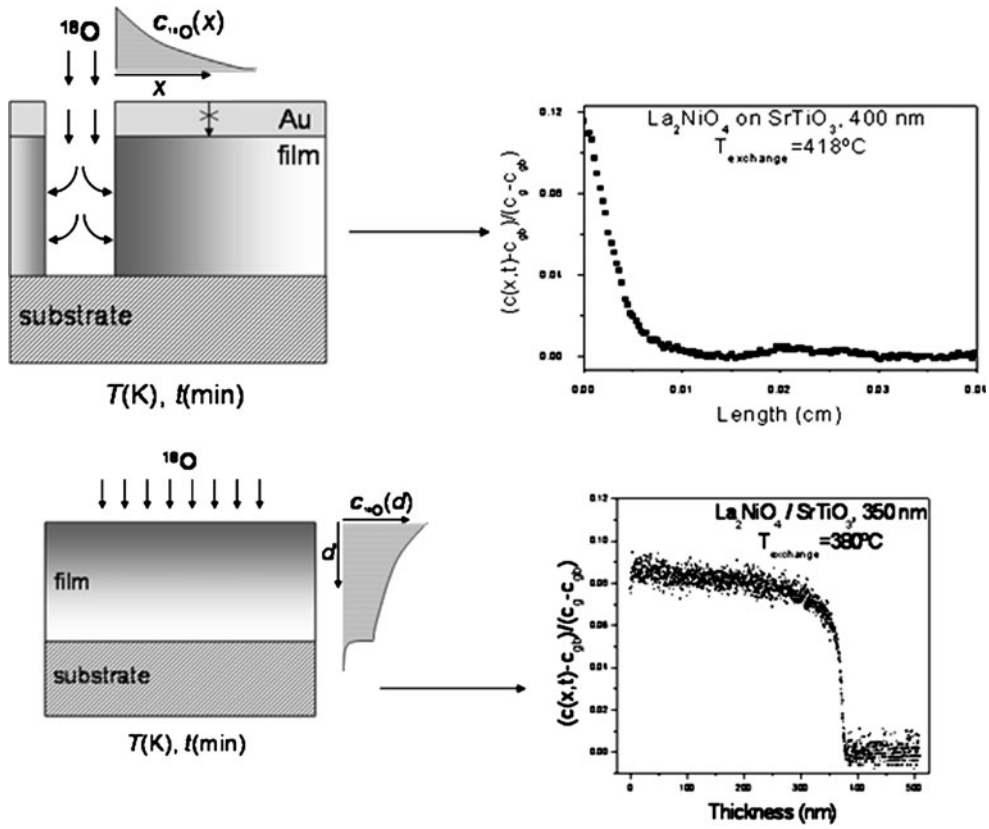

Fig. 5 Diffusion profiles and schematic representation of the experimental determination of anisotropic thin film oxide ion conductivity. Reproduced from Burriel et al. [6]

profiles of only a few nm in depth. Furthermore, the dimension of the sample in the line scan can adversely affect the data obtained as it has to be considered that diffusion fronts can penetrate the sample from all faces, and this may lead to a raised background isotopic concentration. In this circumstance it is essential that the diffusion experiment is designed to optimise the diffusion length and avoid competing diffusion fronts.

Of course the data obtained from these diffusion profiles, either from depth profiles or line scan techniques can be significantly affected by the nature of the diffusion path in the bulk materials, whether species segregate to grain boundaries in polycrystalline samples, or dislocations in single crystals block(or enhance) diffusion. These materials specific parameters can dramatically affect the shape of the diffusion profile, and hence a standard fitting routine using the semi-infinite solution to Fick's 2nd law of diffusion is inadequate. It is of course feasible to fit these data to alternative solutions to the diffusion equation, including tailing functions etc., and a fuller discussion of these possibilities is given in Crank [13].

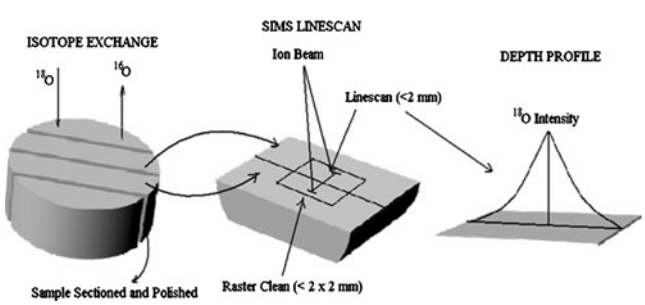

Fig. 6 Schematic of the sample geometry required to obtain diffusion depth profiles from the line scan mode

There is also the possibility of acquiring similar line scan data from ToF-SIMS measurements, although in this instance the method requires the cross-section sample to be surface imaged and the data integrated over a selected area to produce a line scan, as illustrated in Fig. 8 for a sample of the potential electrolyte $La_2Mo_2O_9$. The data from both line scan techniques has been reported previously [14, 15] and found to be in excellent agreement, indicating that the data interpretation is robust.

Diffusion analysis under applied electrical bias

Many of the oxygen tracer measurements of fuel cell materials reported have been carried out under equilibrium conditions as a function of temperature and potentially pO_2 to relate observed behaviour with calculated defect chemistry. However, there have been very few reports of the

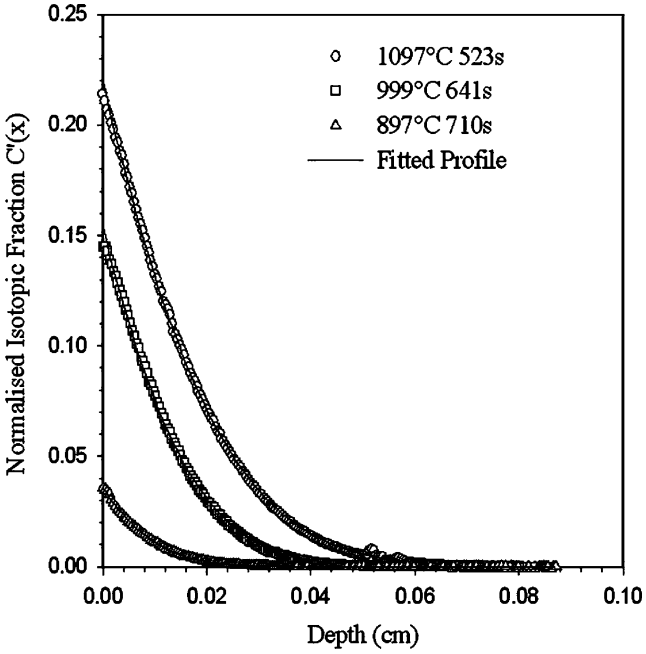

Fig. 7 Typical line scan profiles of ^{18}O penetration into a 9.5% YSZ single crystal [5]

effect of applied electrical bias on the diffusion of oxygen in SOFC materials. One of the few reports is that of Vannier et al. [16] in which a BIMEVOX sample was isotopically exchanged in dry $^{18}O_2$ under small electrical loads. To analyse the effect of applied bias on the oxygen exchange a gold electrode was applied to half of the polished face of the electrolyte sample, with the opposing face fully covered in gold paste and supported on an alumina substrate. Applied currents of 8 and 80 mA were then delivered to the sample during an isotopic exchange anneal and voltages of between 0.5 and 2 V measured. Figure 9 highlights some of the data obtained which indicated that the oxygen exchange reaction now occurring over the surface of the BIMEVOX electrolyte, rather than being confined to triple points. This is apparently associated with local reduction of the vanadium species, giving the electrolyte a local mixed conductivity. Structurally the material is unchanged and the local reduction is fully reversible. From these measurements, it is clear that the exchange behaviour of the material under electrical load is dramatically different from that without applied bias and highlights the need to characterise fuel cell and related materials under realistic operating conditions.

Demanding applications—heterostructured nanomaterials

One of the most exciting recent reports of developments in fast oxide ion conductors has been the apparent enhancement in oxygen mobility in heterostructured materials. Sase et al. [7, 8] reported that in a system with a heterostructure of La_2CoO_4 and $(La,Sr)CoO_3$ a diffusion coefficient greater than either of these components was observed. Following on from this discovery has been the report of Barriocanal et al. [17] where enhanced conductivity was reported in a system of STO/YSZ/STO where the YSZ layer was 1 nm thick. Whilst the former measurements were obtained by SIMS, the latter data were obtained by impedance spectroscopy. These have been a source of interest and controversy, with no unambiguous determination of the oxygen ion conductivity and this presents an ideal opportunity for isotopic labelling and SIMS analysis to resolve this issue. However as discussed by De Souza and Martin [10] these measurements are not trivial, and as yet have only been reported for nanocrystalline ceramic YSZ samples [18] with one preliminary report of the YSZ/STO heterostructure [19]. Future developments of experimental protocols and instrument developments should enable these measurements to be made in the very near future.

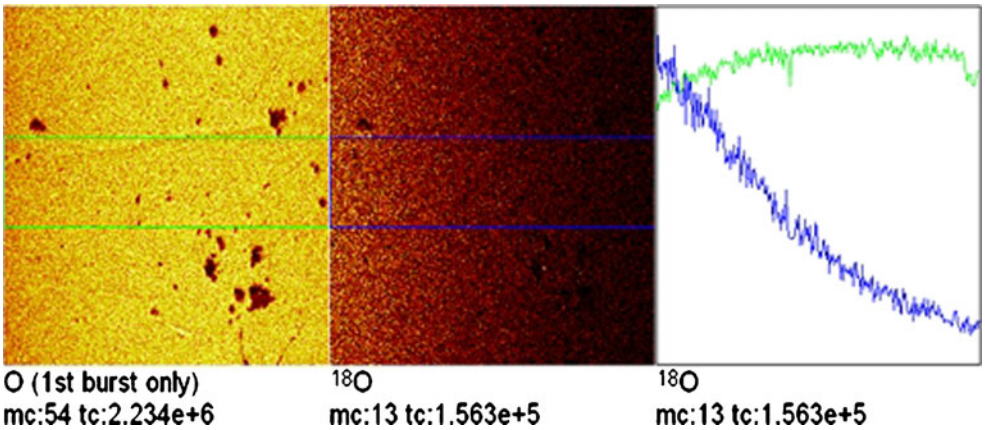

Fig. 8 Example of a line scan depth profile obtained from TOF-SIMS using the surface imaging technique. Isotopic exchange was performed at 700 °C. Highlighted areas on the images are the area integrated to obtain the diffusion profile

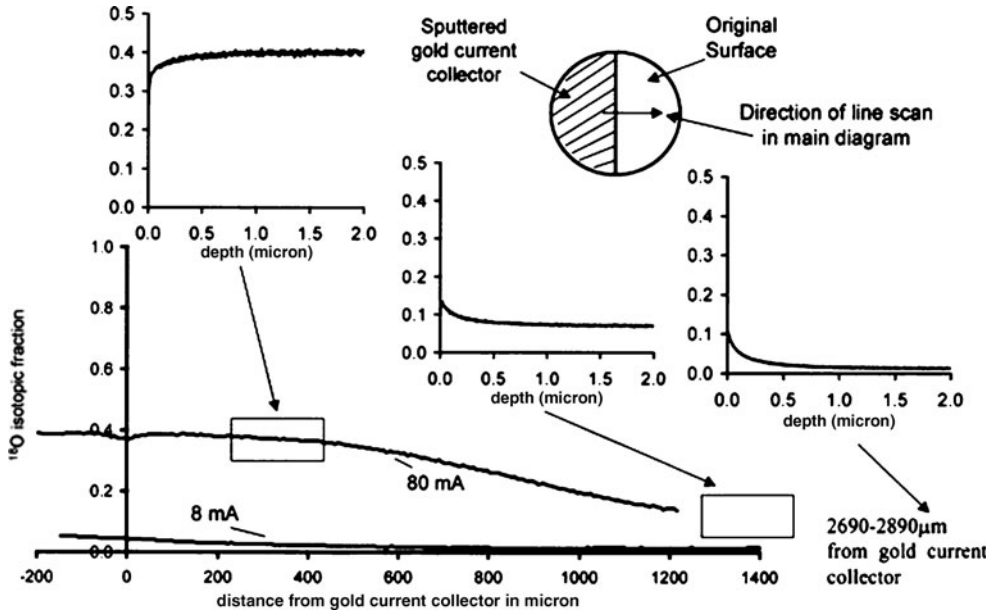

Fig. 9 Diffusion data obtained from a BIMEVOX sample isotopically exchanged under an applied electrical bias. Data highlight the effect of local reduction on the oxygen transport in this electrolyte composition. Reproduced with permission from [16]

Principles and features of LEIS

Low-energy ion scattering

While most surface analytical tools probe an average of many atomic layers, LEIS, also known as ion scattering spectroscopy, has the unique property that it gives the atomic composition of the outer atoms of the surface. This atomic composition plays a crucial role in the adsorption and dissociation of oxygen molecules and can become the rate limiting factor in SOFC and oxygen membranes. In addition to the selective analysis of the outermost atomic layer, high-resolution depth profiling is possible with LEIS.

In LEIS, noble gas ions of a known mass and energy are directed at a sample surface. For the low-energy regime the energy of the incident ions is 0.5–10 keV. An example of an energy spectrum of the backscattered ions is given in Fig. 10. The peaks in this spectrum result from a binary collision of the ions with an atom in the outermost atomic layer. The energy of a peak is determined by conservation of energy and momentum. When an ion of mass m_{ion} and incident energy E_{i} is backscattered over an angle θ by a surface atom of mass m_{at}, the backscattered energy of the ion E_{f} is given by:

$$E_f = E_i \left\{ \left[\cos\theta + \sqrt{\left(r^2 - \sin^2\right)} \right] / (1 + r) \right\}^2 \qquad (7)$$

for $r = m_{\mathrm{at}}/m_{\mathrm{ion}} \geq 1$ and $\theta \geq 90°$.

The energy distribution of the backscattered ions is thus a mass spectrum of the atoms in the outer surface. Backscattering is limited to atoms of a higher mass than that of the noble gas ion, thus only $^3He^+$ and $^4He^+$ ions can be used for the detection of light elements such as oxygen. Since LEIS gives a mass analysis of the atoms, it can distinguish and quantify isotopes like ^{16}O and ^{18}O. The choice of the ion depends on the mass resolution that is required. To separate the heavier elements such as Y and Zr, a heavier noble gas ion such as Ne^+, Ar^+ is used. For the separation of Pt and Au, which are not only heavy but the masses of the isotopes even overlap (Pt, 194–198; Au, 197), the heavy $^{84}Kr^+$ ions were used [20]. For large scattering angles (90–180°) and non-grazing angles, the atomic composition can be quantified, which is done with reference samples. Since there are, in contrast to techniques such as SIMS, in general no matrix effects in LEIS [21], the choice of reference samples is quite wide. The principles and the quantification of LEIS have been reviewed in detail [21], while the application to oxides was reviewed by Brongersma et al. [22].

Figure 11 gives in four snapshots an impression of what happens during an ion–solid collision. After an ion reaches the surface (Fig. 11a) the scattered ion leaves the surface within 10^{-14}–10^{-16} s (Fig. 11b). It takes much longer (10^{-11}–10^{-13} s) before this leads to significant damage (Fig. 11c) and the secondary ions leave the surface (Fig. 11d). This cartoon illustrates that the energy information that the backscattered (LEIS) ion has results from the surface before it is disturbed. This has been verified with molecular dynamics simulations [23]. One should avoid, of course, that another ion hits the same spot. Using a high-sensitivity spectrometer one can use such low ion fluences that this probability is negligible. Since SIMS is based on the analysis of secondary ions, this information relates of course to the sputtered surface.

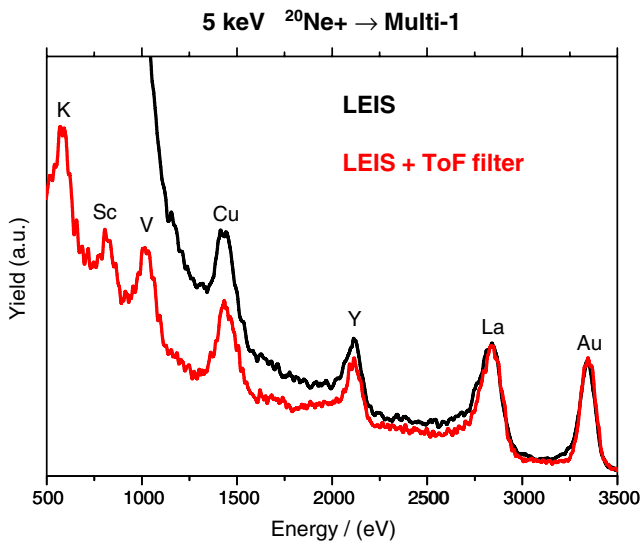

Fig. 10 LEIS energy spectrum of 5 keV $^{20}Ne^{+}$ ions scattered by a multi-component sample. The rising background at low energies is due to secondary ions. It can be removed by time-of-flight filtering (red spectrum), thus enabling the detection and quantification of the lighter elements (K, Sc and V) [24]

On the low-energy side of a peak there is generally an increased background ("tail"), resulting from collisions with that type of atom in deeper layers. The shift to lower energies is due to the extra energy loss along the incoming and outgoing trajectory (Fig. 12). For the heavier elements, the shape of the tail gives an accurate depth profile of that type of atom [24, 25]. Alternatively, LEIS can be combined with a 2nd ion gun for sputter depth profiling, taking advantage of the monolayer sensitivity and ease of quantification of LEIS. The conditions for this are similar to that for depth profiling with SIMS.

On the low-energy side of the energy spectrum (Fig. 10) there is generally an increased (structureless) background due to sputtered ("secondary") ions, the so-called high-energy SIMS ions. The contribution from these ions decreases rapidly with increasing energy. An energy spectrometer analyses, the energy spectrum of the ions irrespective of their mass. Thus, it does not distinguish between backscattered primary ions and secondary ions of the same energy. A high background of secondary ions thus complicates the detection of light elements (lower sensitivity and low scattered ion energy) in the LEIS spectra. In the Qtac equipment [26], it is possible to combine the energy analysis with time-of-flight filtering of the ions. Since, at a given energy, the flight-time depends on the mass of the ion, a time window can be used to select the backscattered ions and reject ions of different masses (Fig. 10). This feature can be very useful in isotopic exchange studies to improve the accuracy of the determination of the ^{16}O and ^{18}O concentrations.

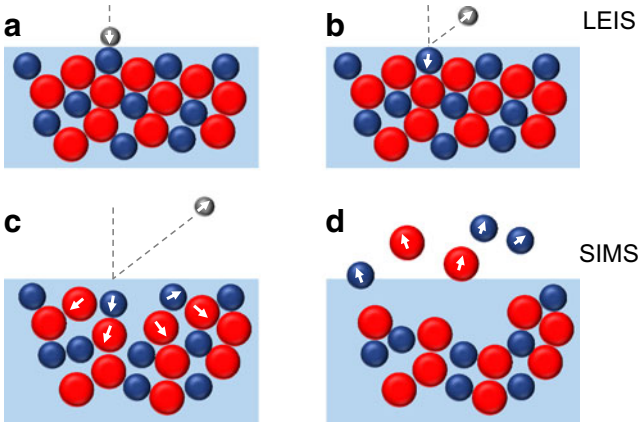

Fig. 11 Snapshots (**a**–**d**) of an ion–solid collision illustrating the LEIS and SIMS processes. Snapshots of an ion–solid collision illustrating the LEIS and SIMS process. The backscattered LEIS ion leaves the undisturbed surface (**b**), while the secondary (SIMS) ions leave much later (**d**)

Sample preparation for LEIS analysis

The preparation of samples for LEIS analysis is similar to that for SIMS. However, due to the extreme surface sensitivity of LEIS extra attention has to be paid to impurities like hydrocarbons [27] and water that will cover the surface of samples that have been transported and stored in the open atmosphere. Although these contaminants will generally not be present during the operating conditions of oxygen membranes and SOFC, they complicate the ex situ analysis. For oxides such as YSZ the thickness of this organic layer is typically 1–2 nm [28]. This contamination can be effectively removed with atomic oxygen at low temperatures [28]. The oxygen atoms are generated in the preparation chamber by an oxygen plasma. To avoid the sputtering action by particles in the plasma that are charged and have a high kinetic energy, these particles are removed from the oxygen atoms flux by a filter. The cleaned sample is transferred under vacuum to the analysis chamber.

Where the sample surface is contaminated with inorganic impurities, these are removed by sputtering. In the older set-ups the primary (LEIS) ion beam is used with an increased ion current. In modern set-ups, like the Qtac [29] a second ion beam producing ions of a few hundred eV is scanned over a larger area, while the primary ion analyses the centre of this area. Since the impurities are generally confined to the outer surface ("The outer surface of polycrystalline oxides"), a very low fluence is sufficient to remove them. The possible damage of the sputter treatment to the sample is annealed by calcination (oxidation at elevated temperature). The CaO-free samples discussed in "Isotopic exchange of pure YSZ surfaces" were produced using oxygen atom cleaning, followed by light sputtering with 1 keV Ar^{+} (maximum dose 1×10^{15} ions/cm^{2}) and

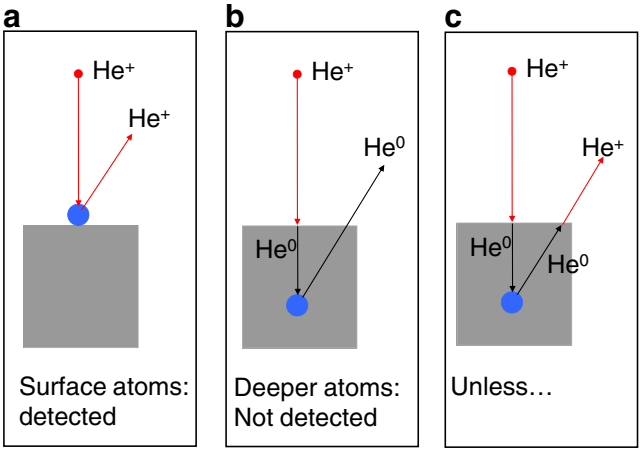

Fig. 12 Cartoon illustrating three possibilities for the backscattering of He^+ ions by a sample, **a** He^+ ion scattered by the outer surface, **b** He^+ ion penetrating in deeper layers is neutralized. An ion that is backscattered by an atom in the deeper layers will not be detected, since the energy analyzer only accepts ions. **c** If after backscattering the He^0 atom encounters an atom such as oxygen, it may be reionized and thus be detected by the analyzer. These ions have not only lost energy during the backscattering process but also during the incoming and outgoing trajectory

calcination at 500 °C. This temperature is high enough to anneal the surface but low enough to prevent thermodynamic equilibrium with the bulk, which would bring again a complete monolayer of CaO to the surface.

LEIS and other analysis techniques such as XPS

For other commonly used surface analysis techniques, the information depth is much larger than for LEIS. For X-ray photoelectron spectroscopy (XPS), it is about 7 nm. By using angle resolved-XPS, this can be improved significantly, but the information depth at grazing angles is still 2 nm [30]. This means that even under those circumstances the signal still results from many (about six) atomic layers. So, the depth resolution does not enable one, for instance, to detect the difference between a complete monolayer coverage and a fractional coverage extending over several atomic layers. The chemical behaviour of a pinhole free barrier layer, is however, very different from that of a layer with partial coverage. The unique monolayer information depth of LEIS is thus essential to understand the surface chemistry and oxygen exchange.

The detected impurities may depend on the used analysis technique. The overlap of the Ca and Zr peaks in XPS makes the detection of Ca impossible in zirconia based materials [31]. Because of the closeness of the atomic masses of Si, Al and of K, Ca these elements are generally not separated in LEIS. Thus if Si and Ca are mentioned, this may also mean that Al and K, respectively, are present at the surface.

The outer surface of polycrystalline oxides

In low-energy ion scattering of polycrystalline ceramics and powders the signal is averaged over many crystal orientations (various surface planes, all azimuths and many angles of incidence). At first sight one might, therefore, expect that a surface analysis would just give the bulk composition of the sample. This is, however, certainly not the case. Lowering of the surface energy is a strong driving force for the segregation (percolation) of certain dopants and impurities to the surface and the grain boundaries. This surface energy originates from the difference in binding of surface and bulk atoms. Since the atoms in the 2nd and deeper layers have almost the same coordination and binding as the bulk atoms, the driving force (and thus the surface enrichment) is mainly restricted to the outer atomic layer.

Lowering of the surface energy can also be the driving force for (re-)crystallization processes in which the crystal plane with the lowest surface energy is favoured at the surface. This outer surface can then serve as a nucleus for the growth of nano-/micro-crystals. Since the energy of a grain boundary is much smaller than a surface energy, it is energetically favourable for a particle to have the lowest possible surface energy, while the extra energy of a grain boundary (crystallographic mismatch) below the surface is easily compensated for. Since the surface energies of the principal surface planes are generally very different, the surface of a small calcined polycrystalline particle may thus be covered almost entirely by planes in which the principal plane is that of the lowest surface energy.

The preparation of ceramic oxide powders involves high-temperature oxidation (calcination). Densification of the material to pellets also requires long term high-temperature sintering. When these ceramics are used in SOFC or as oxygen membranes, they are even exposed to high temperatures during operation. At these temperatures, the atoms in the solid may become very mobile. Thus both the thermodynamics and kinetics are generally favourable for radical changes in the surface composition by surface segregation and (re-)crystallization. This can completely change the atomic composition of the outer surface and the surface properties of the material. This may dramatically alter the oxygen exchange processes at the surface.

Contamination by the gas phase

During operation of an SOFC cell or an oxygen membrane, inorganic gaseous impurities can react with the surface and form a very effective barrier for oxygen exchange and oxygen diffusion. Viitanen et al. [32] report how in permeation experiments the amount of permeated oxygen dropped drastically during the first few minutes of

operation and then remained constant for several weeks. LEIS and XPS showed that the surface of the LSCF membrane was covered with a SiO_2 layer (Fig. 13). The silica originated from siloxanes in the grease of the gas introduction valves. In the O_2/He gas flow, it is transported to the oxygen membrane where it is oxidized at the operation temperature (900 °C) to silica. LEIS showed that close to the air inlet (Fig. 13a) the surface was almost fully covered by silica thus giving an impenetrable film for oxygen. Further away from the inlet (Fig. 13b), the coverage was not complete, thus explaining the remaining transport after a few weeks.

Silica can also be transported via the gas phase in a hydrogen containing humid atmosphere at 1,000 °C. In contact with LSCF a Sr_2SiO_4 compound is formed together with a secondary Fe-rich phase and a $LaCrO_3$-rich grain boundary [33]. Chromium from Fe–Cr interconnects is another well-known impurity that is transported by the gas phase and poisons LSCF cathodes. When Sr is available at the surface, the Cr forms a stable $SrCrO_4$ layer, which gives a rapid performance deterioration [34, 35]. The presence of sulfur in the form of sulfates has also been found as a contaminant [36].

Surface segregation of impurities and dopants

Surface segregation is controlled by the interplay between thermodynamics and kinetics. Although the surface free energy also depends on the neighbouring atoms, the presence in the outer surface of the oxides of especially any alkali, but also those of any alkali earth and silicon, will give low surface energies. When they are embedded in a matrix like YSZ or gadolinium-doped ceria, having a much higher surface energy, there will be a strong driving force for surface segregation of the alkali/alkaline earth and silica. Since the alkali/alkaline earth is also very mobile in an oxidic matrix, their segregation is strong and fast. For example, the surface segregation of Na in ZnO is already observed at temperatures ≥100 °C. Surface enrichment of a factor 10^8 has been observed. Bulk sodium and potassium impurities in the ppb range, which are extremely difficult to detect with any bulk analysis technique, were found with LEIS to give almost a full monolayer of Na_2O/K_2O upon annealing [22, 37]. It is believed that in general for many irreproducible results, where the surface of an oxide plays a role, surface segregation of unknown trace impurities may be responsible.

Perovskites have the general formula $A^{tw}\,B^{oct}\,X_3$, where in the normal perovskites the A cations are twelvefold coordinated by oxygen anions and the B cations are in octahedral sites. LEIS by Fullarton et al. [38] on dense sintered $SmCoO_3$ showed a strong preferential exposure of the A site (Sm), while only 5% of the B site (Co) was visible. Preferential exposure was also found [39] for $BaZrO_3$ and $LiBaF_3$, although it was somewhat less pronounced than in $SmCoO_3$. For oxides with the spinel structure, it is well known that at high-temperatures (re-) crystallization leads to preferential exposure of the plane with the lowest surface energy [40]. For perovskites, the results suggest that the (100)-AO plane, with only A sites, is preferentially exposed at the surface [38].

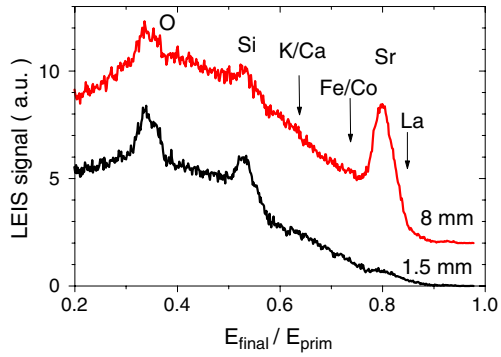

Fig. 13 LEIS spectra of the feed side of an LSCF membrane permeated for about 1,000 h [30], **a** close (1.5 mm) to the inlet the surface is almost fully covered with silica; **b** further away (8 mm) from the inlet, the surface is only partially poisoned by silica. The broad peak around E_f/E_i=0.8 results from Sr and La. No Fe or Co is detected in the outer surface

In perovskites, part of the cations in the A site are often substituted by divalent cations like Sr to increase the number of oxygen vacancies at the surface. Since LEIS gives the atomic fractions of the cations in the outer surface, it showed that mainly Sr and some La covered the surface of a $La_{0.6}Sr_{0.4}Co_{0.2}Fe_{0.8}O_3$ membrane after a 300 h permeation experiment at 900 °C. Only when the surface atoms are removed by sputtering, the B site cations (Co, Fe) become visible [32]. Thus, Co and Fe are not present at the surface and thus cannot participate in the adsorption and dissociation of oxygen molecules at the surface. The strong surface enrichment of Sr leads to a low surface energy, which practically removes the thermodynamic driving force for impurities to segregate to the surface. Surface segregation of impurities is thus generally less pronounced for these LSCF type materials [38] .

It is well known that YSZ contains a variety of inorganic impurities. At the temperatures that are used to prepare YSZ and to operate SOFC, many of these bulk impurities segregate to the surface and grain boundaries where they can have a dramatic effect on the performance of the SOFC. In addition, it has been found that the accumulation at the three-phase boundary can also be electrochemically driven [41]. Typical impurities that segregate are the oxides of Na, Al, Si, K and Ca [41–49].

Using LEIS de Ridder et al. [45] investigated standard YSZ samples made by 3 different suppliers. Even the purest

samples showed a strong segregation of impurities. In all cases a full coverage was reached after a 5 h oxidation at 1,000 °C, but the precise composition of this impurity layer depended on the sample. When a full coverage is reached, the Y and Zr signals have disappeared due to the extreme surface sensitivity of LEIS. In Fig. 14 the 3 keV He^+ spectra are shown for a 10YSZ sample having a relatively clean surface (calcined at 600 °C) and for the same sample fully covered by impurities after calcination at 1,200 °C.

When YSZ is calcined, a pronounced yttria enrichment up to 30 mol% $Y_2O_{1.5}$ (18 mol% Y_2O_3) takes place at the surface or the near-surface [48, 50, 51]. Using LEIS, it was shown that the yttria concentration at the surface increased between 850 and 950 °C, followed by a sharp decrease at 1,000 °C [43, 45, 52]. Above 1,000 °C the surface is fully covered by segregated impurities and the yttria has moved to the layer just below the impurities. The subsurface yttria layer has been confirmed by ToF-SIMS [49].

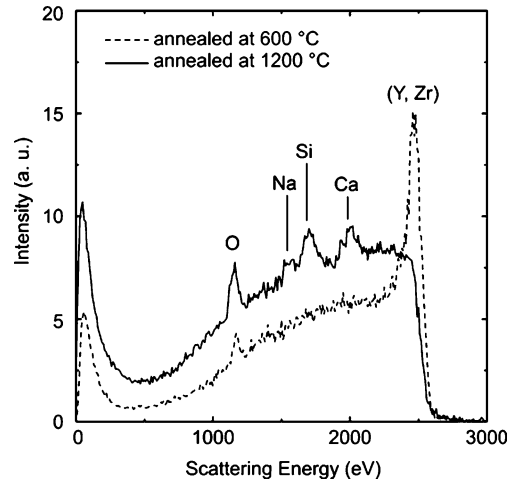

Fig. 14 LEIS spectra (3 keV $^4He^+$) of a 10 mol% Y_2O_3 doped isotopically (^{94}Zr) ZrO_2 sample measured after annealing in oxygen at 600 and 1,200 °C. Y and Zr cannot be separated with He^+ ions and therefore show up as one combined (Y and Zr) peak. After the 1,200 °C anneal the surface is fully covered by segregated impurity oxides (no Y and Zr peak) [43]

LEIS and isotopic oxygen exchange

Since the energy distribution of the backscattered ions is an atomic mass spectrum, LEIS can distinguish the oxygen isotopes in the outer surface. This is illustrated in Fig. 15 for an RCA cleaned silicon wafer that is treated at 1,050 °C for 1 h in 800 mbar oxygen. The spectra have been taken for a scattering angle of 145° with $^4He^+$ ions having a primary energy of 3,000 eV. One spectrum is for a treatment with $^{18}O_2$ and the other with normal oxygen. The peaks are clearly separated and the smooth background enables an accurate determination of the oxygen surface fractions of the exchanged sample. In agreement with Eq. 7, the high-energy onsets of the ^{18}O and ^{16}O are close to their theoretical values of 1,312 and 1,182 eV, respectively.

Site-specific labelling

Cox and Fryberger [53] combined LEIS and isotopic exchange to show for the SnO_2 (110) surface that oxygen atoms in the bridging position are much less stable than oxygen in the in-plane positions. The bridging oxygen could be removed by heating to ≤700 K in vacuum and then preferentially labelled with ^{18}O. Renewed heating proved that the scrambling between bridging and in-plane oxygen is limited.

$Sm_{1-x}Sr_xCoO_3$

Fullarton et al. [38] were the first to combine LEIS and SIMS with oxygen isotopic exchange for perovskites. In a LEIS study of $Sm_{1-x}Sr_xCoO_3$ samples they showed for a sample with x=0.5 that after a 30-min calcination in 1 bar of oxygen at 600 °C strontium is the only cation peak observed (apart from some impurities), see Fig. 16. From a sputter profile it followed that the SrO coverage has only a monolayer thickness. The full coverage implies that Sm and Co cannot take part in the adsorption and dissociation of oxygen molecules from the atmosphere. The samples with x=0, 0.2. 0.4, 0.5 and 0.6 were $^{18}O/^{16}O$ exchanged at a variety of temperatures between 500 and 900 °C. The ^{18}O-concentrations at the surface decreased with increasing Sr concentration in the sample. The ^{18}O concentrations for the LEIS and SIMS experiments showed reasonable agreement, indicating that the ^{18}O-concentration at the surface (LEIS) is comparable to that of the near-surface region (SIMS).

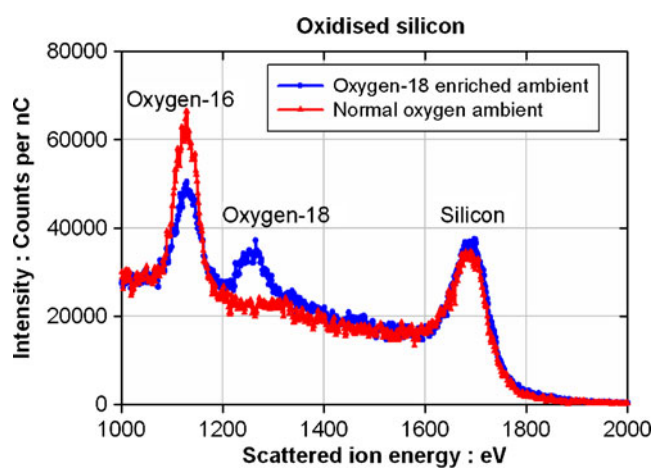

Fig. 15 LEIS spectra for 3 keV $^4He^+$ scattered by a silicon wafer that was oxidized in an oxygen-18 and in a normal oxygen ambient

Isotopic exchange of pure YSZ surfaces

De Ridder et al. [54] studied the isotopic oxygen exchange of high-purity 10YSZ. The surface of the sample, having CaO as its main contaminant, was first cleaned with atomic oxygen, light sputtering and 500 °C calcination (see "Sample preparation for LEIS analysis"). After oxygen exchange with $^{18}O_2$ at temperatures between 250–500 °C the surface concentration and the diffusion profile (using sputtering) were measured with LEIS. The ^{18}O concentration showed a fast decrease with depth for the outer 6 nm (region 1). For 500 °C the surface exchange coefficient k_1= 3.6 (±0.8)×10^{-8} cm/s and the oxygen self-diffusion coefficient D_1=3.0 (±0.8)×10^{-13} cm^2/s.

For larger depths (region 2, 9–15 nm) the ^{18}O fraction becomes almost a constant. Using elastic recoil detection analysis (ERDA) with 35 MeV Cl^- ions the ^{16}O and ^{18}O concentrations were determined up to 1,000 nm deep, thus forming an important addition to the LEIS results. The value for D_2 (1.6±0.4)×10^{-9} cm^2/s in region 2 and in the ERDA region is in agreement with values reported in literature for the oxygen self-diffusion coefficient in cubic YSZ. The much lower value of D_1 is similar to that of monoclinic YSZ. This was taken as evidence for a monoclinic structure. Lower yttria concentrations would stabilise this phase.

Although thermodynamic equilibrium will have been established after 2 h sintering at 1,400 °C, it cannot be excluded that the subsequent removal of the CaO monolayer by sputtering has caused some local damage and compositional change that is not fully restored at the relatively low anneal temperature (500 °C). A higher annealing temperature was not possible to avoid impurity segregation.

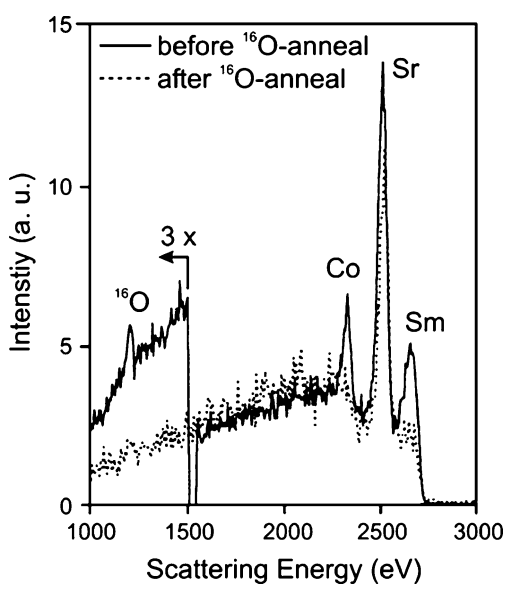

Fig. 16 LEIS spectra (3 keV $^4He^+$) for $Sm_{0.5}Sr_{0.5}CoO_3$ before and after an oxygen anneal of 30 min at 600 °C. After the anneal the Sr (and some impurities) has segregated to the surface, while Co and Sm have disappeared [36]

Influence of CaO contamination on $^{18}O/^{16}O$ exchange

The contamination free surface ("Sample preparation for LEIS analysis") was taken as starting point for the preparation of different CaO surface coverages [54]. They were produced by calcining the sample during a few hours at temperatures up to 1,200 °C. After oxygen exchange at 400 °C the isotopic fraction $^{18}O/(^{16}O+^{18}O)$, as well as the CaO and YSZ surface fractions were determined with LEIS (Fig.17). It shows that with increasing CaO coverage the isotopic fraction drops from 0.52 (uncovered) to close to zero for the complete coverage. The linear decrease of the YSZ coverage with increasing CaO coverage is typical of LEIS (no matrix effects; monolayer sensitivity). With other techniques like XPS (information depth of many atomic layers) and ToF-SIMS (problems with quantification) such a correlation would be impossible. The presence of CaO only reduces the effective surface area for oxygen exchange, not the exchange mechanism [43, 54].

Improved $^{18}O/^{16}O$ exchange by sample modification

The dramatic influence that surface impurities like Ca and Si play in the oxygen exchange [55, 56] has triggered several other groups to develop procedures to produce contamination free surfaces that are stable during long term operation in a SOFC. The easiest would be to use ultra pure YSZ. This would require that the impurity level in the current raw materials (100–1,000 ppm) should be reduced to 1–10 ppm to prevent significant impurity segregation of traditionally processed YSZ [54]. Since this is far from easy, scavengers like CeO_2 [57] and Al_2O_3 [58] have been used for silica. This seems to be partially successful, but can lead to new problems like alumina segregation. Removal of the surface impurities by etching in concentrated HF led to a dramatic improvement, but after the 1st heating cycle the bad conductance returned [59]. Also, one would expect that this solution will not remove the alkali earth like Ca, Sr and Ba, since their fluorides are not very soluble.

In attempts to improve the surface exchange coefficient of YSZ, the surface has been modified by deposition of ultra-thin films and by ion implantation. Another interesting solution to the surface impurity problem is to coat traditionally processed electrolytes with a low-temperature deposited thin film electrolyte. A sputter deposited 100 nm thick YSZ film from a Y_9Zr_{91} metal alloy onto the substrate led to as much as three orders of magnitude improvement in

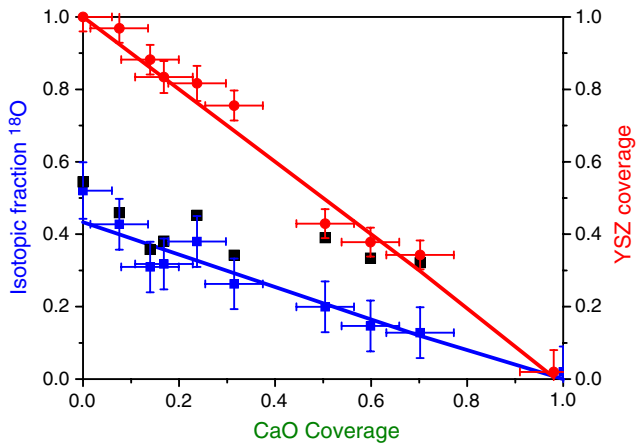

Fig. 17 LEIS shows that the oxygen exchange is prevented by CaO. The YSZ coverage (red circles) is given as a function of the CaO coverage. The blue squares indicate the isotopic fraction $^{18}O/(^{16}O+^{18}O)$. The black squares give the isotopic fractions on the YSZ, if it is assumed that the exchange is only takes place on the YSZ surface and not on the CaO-covered part [52]

the performance of platinum electrodes on this YSZ [59]. The results also confirm the direct connection between surface impurities and electrode performance.

The YSZ surface has also been modified with atomic layer deposition (ALD). The ALD technique enables accurate growth of (sub-)monolayers. Iron oxide was grown with acetylacetonate and oxygen as precursors [60]. Although the Fe diffusion coefficient for the ALD grown iron oxide was significantly lower than that of the implanted iron oxide, the stability was not adequate. It started to dissolve into the bulk at 800–1,000 °C [45, 46].

van Hassel et al. implanted YSZ with a fluence of 8×10^{16} Fe ions/cm^2 of 15 keV [61, 62]. ^{18}O isotope exchange experiments showed that the oxygen exchange rate had improved by at least a factor 30 by the implantation. Although this improvement may be due to the implantation itself, the main cause may well be due to the ion fluence which is so high that its sputtering action will easily have removed all inorganic impurities from the surface. Unfortunately, the improvement was only stable up to 700–800 °C.

In order to obtain a more stable surface modification, Vervoort et al. [63] implanted YSZ with V and W ions of 10 keV. The surface energies of vanadium- and tungsten oxide are much lower than that of iron oxide, while V and W can also exist in several valence states. Although there was a clear oxygen exchange at 700 °C, after a 1,000 °C calcination the LEIS peaks of V, W and YSZ had been suppressed by Na, Ca, while there was no more ^{18}O uptake.

Although these modifications can lower the required operation temperature, further research is needed to identify more stable solutions.

Summary

In this article, we have described the application of two ion beam based techniques to the study of the isotopic exchange of oxygen with oxide materials. The two key parameters that define the kinetics of the exchange process, viz the oxygen tracer diffusion coefficient, D, and the oxygen surface exchange coefficient, *k*, have been explained and the experimental protocols used to obtain these parameters have been described. Whilst these techniques apply to the study of all oxide materials, the materials chosen as illustrations in this article have been materials that display fast oxygen transport for high temperature electrochemical applications in advanced energy conversion systems.

Both SIMS and LEIS are used for the analysis of the surface and near-surface layers of isotopically exchanged oxide materials, but the sensitivity of the two are different. Figure 18 is a schematic that shows the relative information depth and detection range of a number of surface analytical techniques including SIMS and LEIS. From Fig. 18, it is clear that LEIS is able to give information about the elemental composition of the outermost surface layer. Indeed it is also able to give information on the surface oxygen isotopic fraction which is of some interest for the quantification of the isotopic depth profiles. The surface compositional data will be invaluable for the correlation of composition with the surface exchange rates, particularly for the multi-component oxide materials that are now being proposed as the active components in high temperature electrochemical cells. LEIS will also be sensitive to the development of the degradation processes that have been found to occur at, for instance, the cathodes in SOFCs. The degradation is thought to be associated with slow changes

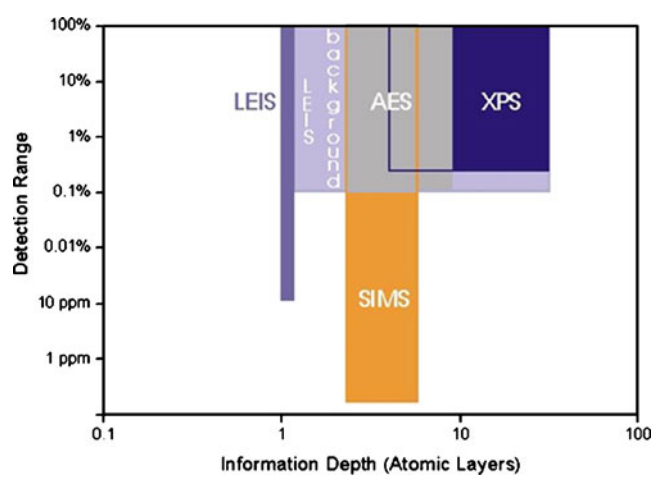

Fig. 18 A comparison of the detection limits and the information depths of some common surface analytical techniques (AES, LEIS, SIMS and XPS). For LEIS, both the detection limit for atoms in the outer surface ("LEIS") and for the in-depth information ("LEIS background") are given

in the surface and subsurface chemistry of the oxide materials under operating conditions [64]. The forte of SIMS for the kind of measurement described in this article is in the depth profiling and cross-sectional imaging of oxygen isotope exchanged materials, mainly to provide accurate determinations of the oxygen self-diffusion coefficient for comparison with the measured electrochemical activity of the materials. SIMS is also able to give a much broader compositional survey over much larger depth ranges that that available from LEIS which is very surface specific. The two techniques are ideally matched to give a wealth of information relevant to the development of high performance, robust and durable materials for advanced electrochemical devices.

Acknowledgements We thank Richard Chater for assistance with the preparation of Fig. 15.

References

1. Berenov AV, Atkinson A, Kilner JA, Bucher E, Sitte W (2010) Solid State Ionics 181:819
2. Opila EJ, Tuller HL, Wuensch BJ, Maier J (1993) J Am Ceram Soc 76:2363
3. Bassat JM, Odier P, Villesuzanne A, Marin C, Pouchard M (2004) Solid State Ionics 167:341
4. Ruiz-Trejo E, Sirman JD, Baikov YM, Kilner JA (1998) Solid State Ionics 113:565
5. Manning PS, Sirman JD, DeSouza RA, Kilner JA (1997) Solid State Ionics 100:1
6. Burriel M, Garcia G, Santiso J, Kilner JA, Chater RJ, Skinner SJ (2008) J Mater Chem 18:416
7. Sase M, Hermes F, Yashiro K, Sato K, Mizusaki J, Kawada T, Sakai N, Yokokawa H (2008) J Electrochem Soc 155:B793
8. Sase M, Yashiro K, Sato K, Mizusaki J, Kawada T, Sakai N, Yamaji K, Horita T, Yokokawa H (2008) Solid State Ionics 178:1843
9. De Souza RA, Chater RJ (2005) Solid State Ionics 176:1915
10. De Souza RA, Martin M (2009) MRS Bull 34:907
11. Haneda H, Sakaguchi I, Ohashi N, Saito N, Matsumoto K, Nakagawa T, Yanagitani T, Yagi H (2009) Mater Sci Tech Lond 25:1341
12. Sakaguchi I, Matsumoto K, Nagata H, Hiruma Y, Haneda H, Takenaka T (2010) Jap J Appl Phys 49:5
13. Crank J (1975) The Mathematics of Diffusion. Oxford University Press, Oxford
14. Liu J (2010) Ph.D. thesis, Department of Materials, Imperial College London, London
15. Liu J, Chater RJ, Hagenhoff B, Morris RJH, Skinner SJ (2010) Solid State Ionics 181:812
16. Vannier RN, Chater RJ, Skinner SJ, Kilner JA, Mairesse G (2003) Solid State Ionics 160:327
17. Garcia-Barriocanal J, Rivera-Calzada A, Varela M, Sefrioui Z, Iborra E, Leon C, Pennycook SJ, Santamaria J (2008) Science 321:676
18. De Souza RA, Pietrowski MJ, Anselmi-Tamburini U, Kim S, Munir ZA, Martin M (2008) Phys Chem Chem Phys 10:2067
19. Cavallaro A, Burriel M, Roqueta J, Apostolidis A, Bernardi A, Tarancon A, Srinivasan R, Cook SN, Fraser HL, Kilner JA, McComb DW, Santiso J (2010) Solid State Ionics 181:592
20. Brongersma HH, Grehl T, Schofield ER, Smith RAP, ter Veen HRJ (2010) Platinum Met Rev 54:81
21. Brongersma HH, Draxler M, de Ridder M, Bauer P (2007) Surf Sci Rep 62:63
22. Brongersma HH, PAC Groenen, JP Jacobs (1994) In: Nowotny J (Ed) Interfaces II. Elsevier, New York. pp. 113
23. Denotter WK, Brongersma HH, Feil H (1994) Surf Sci 306:215
24. Rooij-Lohmann VITA, AW Kleyn, F Bijkerk, HH Brongersma, AE Yakshin (2009) Appl Phys Lett 94
25. Vanleerdam GC, Lenssen KMH, Brongersma HH (1990) Nucl Instrum Meths B 45:390
26. Brongersma HH, Grehl T, van Hal PA, Kuijpers NCW, Mathijssen SGJ, Schofield ER, Smith RAP, ter Veen HRJ (2010) Vacuum 84:1005
27. van der Heide PAW (2002) Surf Interface Anal 33:414
28. de Ridder M, van Welzenis RG, Brongersma HH (2002) Surf Interface Anal 33:309
29. ION-TOF GmbH. Available at: www.iontof.com
30. Bernasik A, Kowalski K, Sadowski A (2002) J Phys Chem Solids 63:233
31. Norrman K, Vels Hansen K, Mogensen M (2006) J Eur Ceram Soc 26:967
32. Viitanen MM, von Welzenis RG, Brongersma HH, van Berkel FPF (2002) Solid State Ionics 150:223
33. Kaus I, Wiik K, Dahle M, Brustad M, Aasland S (2007) J Eur Ceram Soc 27:4509
34. Jiang SP, Zhang S, Zhen YD (2006) J Electrochem Soc 153:A127
35. Chen XB, Zhang L, Jiang SP (2008) J Electrochem Soc 155: B1093
36. Thursfield A, Metcalfe IS (2007) J Membr Sci 288:175
37. Brongersma HH, Buck TM (1978) Nucl Instrum Methods B149:569
38. Fullarton IC, Jacobs JP, van Benthem HE, Kilner JA, Brongersma HH, Scanlon P, Steele BCH (1995) Ionics 1:51
39. Rosink J, JP Jacobs, HH Brongersma (1996) Surfaces, Vacuum, and their Applications: 44
40. Jacobs JP, Maltha A, Reintjes JGH, Drimal J, Ponec V, Brongersma HH (1994) J Catal 147:294
41. Mutoro E, Luerssen B, Gunther S, Janek J (2009) Solid State Ionics 180:1019
42. Backhaus-Ricoult M (2008) Solid State Sci 10:670
43. Brongersma HH, de Ridder M, Gildenpfennig A, Viitanen MM (2003) J Eur Ceram Soc 23:2761
44. Hughes AE, Badwal SPS (1991) Solid State Ionics 46:265
45. de Ridder M, van Welzenis RG, Brongersma HH, Wulff S, Chu WF, Weppner W (2002) Nucl Instrum Methods B 190:732
46. de Ridder M, van Welzenis RG, Brongersma HH, Kreissig U (2003) Solid State Ionics 158:67
47. Schmidt MS, Hansen KV, Norrman K, Mogensen M (2008) Solid State Ionics 179:1436
48. Theunissen G, Winnubst AJA, Burggraaf AJ (1992) J Mater Sci 27:5057
49. Hansen KV, Norrman K, Mogensen M (2006) Surf. Interface Anal 38:911
50. Hughes AE, Sexton BA (1989) J Mater Sci 24:1057
51. Steele BCH, Butler EP (1985) British Ceramic Proceedings. Institute of Ceramics, Stoke-on-Trent
52. de Ridder M, van Welzenis RG, van der Gon AWD, Brongersma HH, Wulff S, Chu WF, Weppener W (2002) J Appl Phys 92:3056
53. Cox DF, Fryberger TB (1990) Surf Sci 227:L105
54. de Ridder M, Vervoort AGJ, van Welzenis RG, Brongersma HH (2003) Solid State Ionics 156:255
55. Bouwmeester HJM, Kruidhof H, Burggraaf AJ (1994) Solid State Ionics 72:185
56. Steele BCH (1995) Solid State Ionics 75:157

57. Wang ZW, Cheng MJ, Dong YL, Zhang M, Zhang HM (2005) Solid State Ionics 176:2555
58. Schmidt MS, Hansen KV, Norrman K, Mogensen M (2008) Solid State Ionics 179:2290
59. Hertz JL, Rothschild A, Tuller HL (2009) J Electroceram 22:428
60. Van Der Voort P, van Welzenis R, de Ridder M, Brongersma HH, Baltes M, Mathieu M, de Ven PC, Vansant EF (2002) Langmuir 18:4420
61. Vanhassel BA, Boukamp BA, Burggraaf AJ (1992) Solid State Ionics 53:890
62. Vanhassel BA, Burggraaf AJ (1991) Appl Phys A 53:155
63. Vervoort AGJ, Scanlon PJ, de Ridder M, Brongersma HH, van Welzenis RG (2002) Nucl Instrum Methods B 190:813
64. Bucher E, W Sitte (2010) Solid State Ionics. DOI:10.1016/j.ssi.2010.01.006
65. De Souza RA, Kilner JA, Walker JF (2000) Mater Lett 43:43